

<sup>1</sup> Context-dependent consequences of lagged effects in  
<sup>2</sup> demographic models

<sup>3</sup> Eric R. Scott<sup>1</sup>, María Uriarte<sup>1</sup>, Emilio M. Bruna<sup>1</sup>

<sup>4</sup> <sup>1</sup>Department of Wildlife Ecology and Conservation, University of Florida, Gainesville,  
<sup>5</sup> Florida 32611-0430 USA

<sup>6</sup> <sup>2</sup>Department of Ecology, Evolution and Environmental Biology, Columbia University 1200  
<sup>7</sup> Amsterdam Avenue, New York, New York 10027 USA

<sup>8</sup> <sup>3</sup>Center for Latin American Studies, University of Florida, Gainesville, Florida 32611-5530  
<sup>9</sup> USA

<sup>10</sup> <sup>4</sup>Biological Dynamics of Forest Fragments Project, INPA-PDBFF, CP 478, Manaus,  
<sup>11</sup> Amazonas 69011-970 Brazil

<sup>12</sup> (draft: 28 October 2025)

<sup>13</sup>

## Abstract

<sup>14</sup> Text of 150 words max summarizing this amazing paper.

<sup>15</sup> **Keywords:** demography, environmental stochasticity, integral projection models,

<sup>16</sup> lagged effects, structured population models, population dynamics

<sup>17</sup> **Manuscript elements:** Figures 1-4, Tables 1-6

<sup>18</sup> **Manuscript type:** e-note

19

## Introduction

20 Current environmental conditions can have immediate effects on the growth, survival, or  
21 reproduction of long-lived organisms. However, there is mounting evidence for potential  
22 delays of months or even years between current environmental conditions and resulting  
23 changes in demographic vital rates. These *Lagged Effects*, also known as *Delayed*  
24 *Life-history Events* (i.e. DLHEs, Beckerman et al. 2002), can simultaneously affect an  
25 entire cohort (e.g., all juveniles hatching during a period of scarcity will have delayed  
26 maturation) or only a subset of the population (e.g., cold winter temperatures reduce  
27 flowering by small trees but not large ones). Moreover, the temporal delay between an  
28 environmental event and changes in demographic vital rates depends on both the intensity  
29 of the event and its timing relative to the underlying physiological processes (Criley and  
30 Lekawatana 1994; Evers et al. 2021). For example, a drought during the early stages of  
31 gestation or floral bud formation might have a much larger impact on the number of fruits  
32 or offspring produced than one at a later stage of the reproductive process. The delay or  
33 intensity of lagged effects can also be location- or habitat-specific, with individuals in some  
34 sites or habitats buffered against, or able to recover more quickly from, the delayed effects  
35 of environmental variation.

36 Because Lagged Effects are often directly linked to reproduction and survival, it has  
37 been argued they could have major but underappreciated consequences for population  
38 dynamics (Beckerman et al. 2002). While recent studies suggest this could indeed the case  
39 (e.g., Williams et al. 2015; Molowny-Horas et al. 2017; Tenhumberg et al. 2018), efforts to  
40 test this hypothesis are rare. (Metcalf et al. 2015). In part this is because empirical tests  
41 of putative lagged effects are challenging to design, implement, and maintain (Kuss et  
42 al. 2008). While one could conceivably use observational data to detect lagged effects,  
43 doing so requires long-term data on both the putative lagged effect (e.g., reduced  
44 probability of flowering) and its potential environmental drivers (e.g., drought during early

45 floral development), and such coupled data sets are rare (*sensu* Evers et al. 2021). In  
46 addition, the methods for both identifying lagged effects and modeling their demographic  
47 impacts can be challenging to implement. For example, many of the potentially applicable  
48 statistical methods have stringent assumptions and data requirements rarely met by  
49 ecological data (Metcalf et al. 2015), while the including complex biological processes in  
50 demographic models can render them less tractable or amenable to analysis using currently  
51 available tools. Addressing these challenges is a major undertaking, and the value of doing  
52 so will depend on the effort required vs. the potential consequences of failing to consider  
53 lagged effects — consequences that range from overestimating projections of population  
54 growth rate (i.e.,  $\lambda$ ) in a conservation setting to drawing invalid conclusions regarding  
55 support for the predictions of ecological or evolutionary theory.

56 Integral Projection Models (i.e., IPMs) are an important and widely used tool for  
57 studying demography and population dynamics (Ellner and Rees 2006; Rees and Ellner  
58 2009; Rees et al. 2014). Their flexibility, in concert with a rapidly growing suite of  
59 software, data, and other resources (Salguero-Gómez et al. 2015; Ellner et al. 2016; Levin  
60 et al. 2021), have facilitated their use to study a wide range of topics in ecology, evolution,  
61 and conservation (Morris and Doak 2002; Crone et al. 2011; Ellner et al. 2016).

62 Mathematical and statistical advances (e.g., Williams et al. 2012; Brooks et al. 2019) have  
63 rapidly expanded the scope of questions and biological processes that can be investigated  
64 with these models (e.g., Metcalf et al. 2015; Ellner et al. 2016; Rees and Ellner 2016). Here  
65 we test predictions for how including lagged effects in Integral Projection Models will  
66 influence projections of  $\lambda$  and population structure.

67 We have previously shown that the effects of precipitation extremes on the  
68 demographic vital rates of an Amazonian understory herb (*Heliconia acuminata*,  
69 Heliconiaceae) can be delayed up to 36 months (Scott et al. 2022), with the presence and  
70 duration of these lagged effects varying by vital rate and habitat (i.e., continuous forest  
71 vs. forest fragments). We parameterized three classes of Integral Projection Models — a

72 deterministic IPM, a stochastic IPM, and a stochastic IPM with lagged effects of  
73 precipitation on vital rates — for populations in these two habitat types to test the  
74 following predictions from demographic theory (Tuljapurkar 1990; Caswell 2001): (i)  
75 projections of  $\lambda$  from deterministic models would be higher than those of stochastic models,  
76 and that (ii)  $\lambda$  is lower for Forest Fragment than Continuous Forest populations regardless  
77 of model, but the difference between the two habitats is greatest for the IPM with lagged  
78 effects.

79 **Methods**

80 ***Study System and Demographic Data***

81 *Heliconia acuminata* (Heliconiaceae) is a perennial, self-incompatible monocot that is  
82 distributed throughout much of the Amazon basin (Kress 1990). While some *Heliconia*  
83 species grow in large aggregations on roadsides, gaps, and in other disturbed habitats,  
84 others, including *H. acuminata*, grow primarily in the forest understory (Kress 1983;  
85 Ribeiro et al. 2010). Understory *Heliconia* species produce fewer flowers and are pollinated  
86 by traplining hummingbirds (Stouffer and Bierregaard 1996; Bruna et al. 2004). The  
87 models and analyses here are based on 11 years (1998-2009) of demographic data collected  
88 on >8500 *H. acuminata* found at Brazil's Biological Dynamics of Forest Fragments Project  
89 (BDFFP), located ~70 km north of Manaus, Brazil. The BDFFP reserves include both  
90 continuous forest and forest fragments that range in size from 1-100 ha. These fragment  
91 reserves were originally isolated in the early 1980's by the creation of cattle pastures, with  
92 the secondary growth surrounding them periodically cleared to ensure their continued  
93 isolation. The habitat in all sites is non-flooded lowland rain forest with rugged  
94 topography. A complete summary of the BDFFP and its history can be found in  
95 Bierregaard et al. (2001).

96 A complete description of our demographic methods, data, and analyses to date can be

97 found in Bruna et al. (2023). Briefly, in 1997–1998 a series of 5000 m<sup>2</sup> plots were  
98 established in the BDFFP reserves: N=6 in Continuous Forest and N=4 in 1-ha Forest  
99 Fragments (i.e., CF and FF, respectively). All of the *Heliconia acuminata* in these plots  
100 were marked and measured; the plots were censused annually, at which time a team  
101 recorded the size of surviving individuals, marked and measured new seedlings, and  
102 identified any previously marked plants that died. Each plot was also surveyed 4-5 times  
103 during the flowering season to identify reproductive plants. These surveys were  
104 complemented by data on the number of fruits per flowering plant (Bruna 2021) and seeds  
105 per fruit (Bruna 2014) that were collected outside of the demographic plots to avoid  
106 altering within-plot recruitment. We also conducted experiments to quantify the  
107 probability of seed germination and seedling establishment in both forest fragments and  
108 continuous forest (Bruna 1999, 2002).

109 The rainy season in our sites is typically from late December through late May.  
110 *Heliconia acuminata* in our site begin flowering early in the rainy season and most  
111 reproductive plants produce a single inflorescence (range = 1–7) with 20–25 flowers (Bruna  
112 and Kress 2002). Fruits mature April-May and have 1–3 seeds per fruit ( $\bar{x} = 2$ ) that are  
113 dispersed by a thrush and several species of manakin (Uriarte et al. 2011). Dispersed seeds  
114 germinate approximately 6 months after dispersal at the onset of the subsequent rainy  
115 season, with rates of germination and seedling establishment higher in continuous forest  
116 than forest fragments (Bruna 1999, 2002). On average, plots in CF also had more than  
117 twice as many plants as the plots in 1-ha fragments (CF: median = 788, range = 201-1549;  
118 1-ha: median = 339, range = 297-400).

### 119 ***Construction of Integral Projection Models***

120 We projected the growth rate and structure of *Heliconia acuminata* with three classes of  
121 IPMs: Deterministic, Stochastic, and Stochastic with Lagged Environmental Effects. Each  
122 of these IPMs required different functional forms of the underlying vital rate functions used

123 to describe the *H. acuminata* life cycle (Figure 1). All models were density-independent,  
 124 with the deterministic model serving as the foundation for the more complex models. Our  
 125 modeling workflows were managed using the `targets` R package (Landau 2021); in  
 126 addition to ensuring reproducibility this allowed us to track computational time spent  
 127 processing and analyzing each class of IPM.

128 **(1) Deterministic IPM:** In this model the size and structure of a population in year  
 129  $t + 1$  is determined by the survival and growth of plants alive in year  $t$  (Equation 1) plus  
 130 the number of new seedlings that entered the population (Equation 2).

$$n(z', t + 1) = R(z')n_s(t) + \int_L^U P(z', z)n(z, t) dz \quad (1)$$

$$n_s(t + 1) = \int_L^U F(z)n(z, t) dz \quad (2)$$

131 Equation 1 has two components. The first is the sub-kernel  $P(z', z)$ , which describes  
 132 the size-dependent survival and growth/regression of mature plants (Equation 3):

$$P(z', z) = s(z)G(z', z) \quad (3)$$

133 The second is sub-kernel  $R(z')$ , which describes the survival of seedlings established in year  
 134  $t$  and their size when entering the mature plant population in year  $t + 1$  (Equation 4):

$$R(z') = s_s G_s(z') \quad (4)$$

135 Note that in Equation 4 both the probability that new seedlings survive their first year,  $s_s$ ,  
 136 and their size at the end of this year,  $G(z', z)$ , are size-independent. IPMs can include  
 137 transitions between individuals from a discrete state to a continuous one (i.e., from  
 138 ‘seedling’ to ‘mature plant of size  $z'$ ; Ellner et al. 2016); we treat seedlings as a distinct  
 139 and discrete category because they have lower survival and growth in their first year than

140 comparably sized plants (Bruna 2003; Scott et al. 2022).

141 The number of new seedlings entering the population in year  $t + 1$  is a function of the  
142 number of mature plants in year  $t$  and a sub-kernel describing the size-dependent fecundity  
143 of these individuals (Equation 5):

$$F(z) = p_f(z)f(z)g \quad (5)$$

144 Both the probability that a mature plant will flower,  $p_f(z)$ , and the number of seeds a  
145 flowering plant will produce,  $f(z)$ , are size-dependent. All seeds germinate and establish as  
146 seedlings with probability  $g$ .

147 We used the annual census data (Bruna 2003) to fit the deterministic vital rate  
148 functions for growth, survival, and flowering in each habitat type (i.e., Fragments,  
149 Continuous Forest; the data from all plots within a habitat class were pooled to create a  
150 single ‘summary population’ for the CF and FF habitats (Bruna 2003). For established  
151 plants these were modeled as a smooth function of size in the previous census with  
152 generalized additive models (GAMs) fit with the `mgcv` package (Wood 2011) for the R  
153 statistical programming language (R Core Team 2020). For consistency, seedling survival  
154 and growth were also modeled using GAMs, but without size in the previous census as a  
155 predictor (i.e. ‘intercept-only’ models). For growth models a scaled t family distribution  
156 provided a better fit to the data than a Gaussian fit, as the residuals with a simple  
157 Gaussian model were Leptokurtic. To model size-specific fecundity we used the data on  
158 fruits per flowering plant (Bruna 2021), seeds per fruit (Bruna 2014), and the  
159 experimentally-derived estimates of seed germination and seedling establishment (Bruna  
160 1999, 2002).

161 **(2) Stochastic IPMs:** To include temporal stochasticity in our IPMs we included a  
162 random effect of year. This was done using a factor-smooth interaction that allowed the  
163 functional form of the relationship between plant size and vital rates to vary among

164 transition years (Figure 1). We generated kernels for every transition year using the  
165 long-term survey data (Bruna et al. 2023) and random smooths for year. We then  
166 randomly selected one of these sets of kernels to use in each iteration of the IPM. This  
167 procedure is equivalent to ‘*kernel resampling*’ (*sensu* Metcalf et al. 2015) or matrix  
168 selection for matrix population models (Caswell 2001; Boyce et al. 2006).

169 **(3) Stochastic IPMs with lagged effects of precipitation on vital rates:** We  
170 explicit modeled the lagged effects of precipitation extremes on vital rates using the  
171 procedure described in Scott et al. (2022). Briefly, we first calculated the Standardized  
172 Precipitation Evapotranspiraton Index (i.e., SPEI) for our study site using a published  
173 gridded dataset based on ground measurements (Xavier et al. 2016). After we fit vital rate  
174 models using the long-term survey data (Figure 1), we modeled delayed effects of SPEI  
175 with Distributed Lag Non-linear Models (i.e., DLNMs) with a maximum lag of 36 months  
176 (Scott et al. 2022). To iterate these parameter-resampled IPMs (*sensu* Metcalf et al. 2015)  
177 we first created a random sequence of SPEI values by sampling years of the observed  
178 (monthly) SPEI data. For every year we then calculated a lag of 36 months from the  
179 month in which that year’s census was completed. These values were then used to predict  
180 the fitted values from vital rate models, which generated different kernels for each iteration  
181 of the IPM. The kernels of successive iterations are not entirely independent — the SPEI  
182 values used to calculate vital rates include values used in the previous two iterations — but  
183 they are ergodic.

184 All IPMs were constructed and iterated using the `ipmr` package (Levin et al. 2021) for  
185 the R statistical programming language (R Core Team 2020). The IPMs used 100  
186 meshpoints and the midpoint rule for calculating kernels. For each type of IPM we iterated  
187 the model for 1000 time steps, but discarded the first 100 time steps to omit transient  
188 effects. Stochastic growth rates ( $\lambda_s$ ) were calculated as the average  $\ln(\lambda)$  from each time  
189 step (Caswell 2001) and then back-transformed to allow for direct comparison with  
190 projections of  $\lambda$  from deterministic models. The initial starting vector primarily influences

191 a population's transient dynamics; we therefore used the distribution of established plant  
192 sizes and proportion of seedlings in the full demographic data set as the initial population  
193 vector for all models.

194 Finally, We estimated the 95% confidence intervals for each IPMs projections of  $\lambda$ . To  
195 do so we first created 500 populations for each habitat type by sampling individual plants  
196 with replacement (i.e., bootstrapping) until the population size of each matched that of the  
197 initial population vector. We then re-fit the vital rate models for growth, survival, and  
198 flowering for each of these bootstrapped population and constructed new IPMs for each  
199 population as above (the models for germination and establishment rate, fruits per  
200 flowering plant, and seeds per fruit were not refit because these were estimated using  
201 different data sets). The projections of  $\lambda$  for the new populations were then used to  
202 estimate the upper and lower 95% bias-corrected percentile intervals (Caswell 2001; Manly  
203 2018).

204 ***Statistical analyses***

205 **Comparison of  $\lambda$  in Continuous Forest and Forest Fragments**

206 To determine if the deterministic projections of  $\lambda$  for Continuous Forest and Forest  
207 Fragment populations were significantly different we used the randomization test procedure  
208 described by Caswell (2001). Briefly, we randomly assigned plants with their demographic  
209 history among two populations,  $R_1$  and  $R_2$ , that were equal in size to the original CF and  
210 FF populations. We then calculated  $\lambda^{R_1}$ ,  $\lambda^{R_2}$ , and the absolute value of the difference  
211 between the two (i.e.,  $\theta$ ). This was repeated  $N = 1000$  times, after which we determined  
212 the proportion of simulations in which  $\theta$  was greater than the observed difference between  
213  $\lambda^{CF}$  and  $\lambda^{FF}$  (i.e.,  $P[\theta \geq \theta_{obs}]$ ).

214 We used a Generalized Linear Model to compare the projections of  $\lambda$  from the two  
215 stochastic IPMs. We modelled the lambda as a function of IPM type (kernel-resampling vs  
216 parameter-resampling) and Habitat (continuous forest vs. fragments), and the interaction

217 of IPM type and Habitat. Because the response variable ( $\lambda$ ) was continuous we used the  
218 Gaussian distribution with the identity link function in our model. We verified the model  
219 assumptions by plotting residuals versus fitted values.

## 220 Population Structure

221 Finally, we compared the structure of populations through the first 250 time steps in each  
222 habitat by each of the stochastic IPMs (i.e, kernel- vs. parameter-resampling). At each  
223 time step, we assigned the individuals to one of four stage classes based on plant size,  
224 probability of survival, and probability of reproduction (see Table Table 3). We then  
225 calculated the proportion of the population that was in each stage class in each habitat for  
226 each IPM type. Comparing the means and variances of these proportions will allow us to  
227 determine (1) if the two IPMs project different population structures over time, (2) if the  
228 population structure for a given IPM is consistent across habitat type. Because  
229 Shapiro-Wilk tests indicated that the distributions of proportions were not normally  
230 distributed, we used the non-parametric Ansari-Bradley Test to compare the distribution of  
231 proportions in each habitat x stage combination. These analyses were conducted using the  
232 R packages `rstatix` and `vartest`, respectively (Kassambara 2023; Cosar and Dag 2024).

## 233 Results & Discussion

234 All IPMs projected higher population growth rates for *Heliconia acuminata* populations in  
235 Continuous Forest than for those in Forest Fragments (Table 2, Table 6). The differences  
236 between  $\lambda^{CF}$  and  $\lambda^{FF}$ , which ranged from 1.19-2%, were significant for both deterministic  
237 ( $P[\theta \geq \theta_{obs}] = 0$ , N = 1000 randomization) and stochastic IPMs (Table 6). There were also  
238 significant effects of IPM Type, Habitat, and their interaction on  $\lambda$  (Table 6). Because  
239 stochasticity is predicted to reduce population growth rates (Tuljapurkar et al. 2003; Doak  
240 et al. 2005; Metcalf et al. 2015), we were surprised to find that deterministic  $\lambda$  was nearly  
241 identical to the average  $\lambda$  from kernel-resampled IPMs (Figure 3). However, we did see

reductions in population growth rate when including lagged effects in IPMs: on average the projections of  $\lambda$  from these models were 1.5-2% lower, with 70-76% of the values below deterministic  $\lambda$  (Figure 3). The IPMs with lagged effects also appear to be more accurate — the underlying vital rate models for IPMs with lagged effects all had the best fit to the survey data ( $dAIC = 0$ , Table 1).

Including lagged effects in IPMs also resulted in significantly less predictable projections of population structure, both within (Figure 2 A) and across habitats (Figure 2 B, Table 4). This variability is particularly notable in forest fragments (Figure 4, Table 5), where we have previously shown lagged effects have very large impacts on growth and survival (Scott et al. 2022). The deterministic IPM for Continuous Forest projected slightly more of the smallest and largest plants than the one for Forest Fragments. In other words, populations in forest fragments had proportionately less recruitment and fewer individuals growing into the larger, reproductive size classes (Bruna and Oli 2005). This shift towards intermediately sized, pre-reproductive plants in forest fragments is even more dramatic when using the parameter-resampled stochastic IPM (Figure 2 B).

What are the implications of these results for the use of IPMs to study plant demography? First, they suggest that failing to include lagged effects in models could significantly underestimate the growth rate of populations. While relative differences in projections of  $\lambda$  may be sufficient for some tests of theory, the actual value of projections may be critical in conservation or management settings. For example, they could be used to identify which populations face the greatest risk of extinction (e.g.,  $\lambda = 0.99$  vs.  $\lambda = 1.01$ ) or, because even small differences in  $\lambda$  can have major short-term consequences for population dynamics (e.g.,  $\lambda = 1.01$  vs.  $\lambda = 1.02$ ), be used to choose among alternative management strategies. Moreover, including lagged effects in models could be especially critical for studies assessing the effects of climate change, given many DLHE are climate driven.

That said, there is a cost to including lagged effects in demographic models, even when

269 doing so is conceptually appropriate or if the outcome is potentially more accurate. While  
270 Deterministic and Kernel-resampled Stochastic IPMs took only ~0.02 and ~0.07 min to  
271 iterate (respectively), the Stochastic IPMs with using parameter-resampled kernels and  
272 lagged effects took ~87.12 min. This is largely due to the required computational resources  
273 and algorithms (i.e., `predict()`), which are much slower for Generalized Additive Models  
274 with 2D smooths because of the much higher number of knots than for the GAMs used in  
275 Deterministic and Kernel-resampled IPMs. Advances in computational power and access to  
276 high-performance computing resources could lower this temporal and computational cost.

277 It is important to emphasize, however, that computational power cannot compensate  
278 for limited data. Detecting lagged effects and evaluating their consequences requires  
279 long-term demographic data — data that are only available for a relatively small number  
280 of species, few of which are in the tropics (Bruna et al. 2009; Römer et al. 2024). The  
281 increasing evidence that lagged effects are ubiquitous, and that they can have major  
282 demographic impacts, underscores the need to support the collection of such long-term  
283 data, the complementary development of experimental and statistical approaches to  
284 disentangling lagged effects, and community driven efforts to identify priority or model  
285 systems for in-depth investigation.

## 286 Acknowledgments

287 We thank \_\_\_\_\_, \_\_\_\_\_, and \_\_\_\_\_ anonymous reviewers for helpful discussions and  
288 comments on the manuscript. We also thank Sam Levin for his help with the `ipmr` package.  
289 Financial support for collecting the demographic data used in this study was provided by  
290 the U.S. National Science Foundation (awards INT 98-06351, DEB-0309819,  
291 DEB-0614149,DEB-0614339, and DEB-1948607). This article is publication no. \_\_\_\_\_ in  
292 the BDFFP Technical series. The authors declare no conflicts of interest.

293

## CRediT Statement

294 ERS contributed to the conceptualization, methodology, formal analysis, and led the  
295 writing of the original draft. EMB contributed to the conceptualization, methodology,  
296 writing, and, acquired funding.

297

## Data Availability Statement

298 Data and R code used in this study are archived with Zenodo at (*doi and url to be added*  
299 *on acceptance*).

300

## Literature Cited

- 301 Beckerman, A., T. G. Benton, E. Ranta, V. Kaitala, and P. Lundberg. 2002. Population  
302 dynamic consequences of delayed life-history effects. *Trends in Ecology & Evolution*  
303 17:263–269.
- 304 Bierregaard, R. O., C. Gascon, T. E. Lovejoy, and R. Mesquita, eds. 2001. Lessons from  
305 Amazonia: The ecology and conservation of a fragmented forest. Yale University Press,  
306 New Haven.
- 307 Boyce, M., C. Haridas, C. Lee, and The Stochastic Demography Working Group. 2006.  
308 **Demography in an increasingly variable world.** *Trends in Ecology & Evolution* 21:141–148.
- 309 Brooks, M. E., K. Kristensen, M. R. Darrigo, P. Rubim, M. Uriarte, E. M. Bruna, and B.  
310 M. Bolker. 2019. **Statistical modeling of patterns in annual reproductive rates.** *Ecology*  
311 100:e02706.
- 312 Bruna, E. M. 1999. **Seed germination in rainforest fragments.** *Nature* 402:139.
- 313 ———. 2002. **Effects of forest fragmentation on *Heliconia acuminata* seedling recruitment**  
314 **in central Amazonia.** *Oecologia* 132:235–243.
- 315 ———. 2003. **Are plant populations in fragmented habitats recruitment limited? Tests**  
316 **with an Amazonian herb.** *Ecology* 84:932–947.
- 317 ———. 2014. **Dataset: *Heliconia acuminata* seed set (seeds per fruit).** Figshare doi:  
318 10.6084/m9.figshare.1273926.v2.

- 319 ———. 2021. Dataset: Leaf number, leaf area, shoot number, and height of reproductive
- 320 *H. Acuminata*. Zenodo <https://doi.org/10.5281/zenodo.5041931>.
- 321 Bruna, E. M., I. J. Fiske, and M. D. Trager. 2009. Habitat fragmentation and plant
- 322 populations: Is what we know demographically irrelevant? Journal of Vegetation Science
- 323 20:569–576.
- 324 Bruna, E. M., and W. J. Kress. 2002. Habitat fragmentation and the demographic
- 325 structure of an Amazonian understory herb (*Heliconia acuminata*). Conservation Biology
- 326 16:1256–1266.
- 327 Bruna, E. M., W. J. Kress, F. Marques, and O. F. da Silva. 2004. *Heliconia acuminata*
- 328 reproductive success is independent of local floral density. Acta Amazonica 34:467–471.
- 329 Bruna, E. M., and M. K. Oli. 2005. Demographic effects of habitat fragmentation on a
- 330 tropical herb: Life-table response experiments. Ecology 86:1816–1824.
- 331 Bruna, E. M., M. Uriarte, M. R. Darrigo, P. Rubim, C. F. Jurinitz, E. R. Scott, O. Ferreira
- 332 da Silva, et al. 2023. Demography of the understory herb *Heliconia acuminata*
- 333 (Heliconiaceae) in an experimentally fragmented tropical landscape. Ecology 104:e4174.
- 334 Caswell, H. 2001. Matrix population models: Construction, analysis, and interpretation.
- 335 Sinauer Associates, Sunderland.
- 336 Cosar, G., and O. Dag. 2024. Vartest: Tests for variance homogeneity.
- 337 Criley, R., and S. Lekawatana. 1994. Year around production with high yields may be a

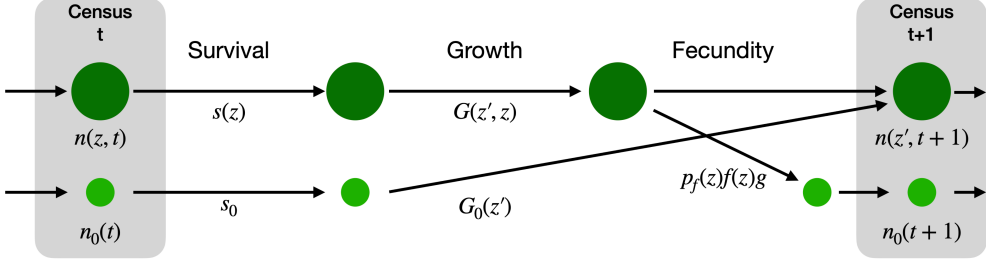
- 338 possibility for *Heliconia chartacea*. Acta Horticulturae 397:95–102.
- 339 Crone, E. E., E. S. Menges, M. M. Ellis, T. Bell, P. Bierzychudek, J. Ehrlen, T. N. Kaye, et  
340 al. 2011. How do plant ecologists use matrix population models? Ecology Letters 14:1–8.
- 341 Doak, D. F., W. F. Morris, C. Pfister, B. E. Kendall, and E. M. Bruna. 2005. Correctly  
342 estimating how environmental stochasticity influences fitness and population growth. The  
343 American Naturalist 166:E14–E21.
- 344 Ellner, S. P., D. Z. Childs, and M. Rees. 2016. Data-driven modelling of structured  
345 populations: A practical guide to the integral projection model. Springer Science+Business  
346 Media, New York, NY.
- 347 Ellner, S. P., and M. Rees. 2006. Integral projection models for species with complex  
348 demography. American Naturalist 167:410–428.
- 349 Evers, S. M., T. M. Knight, D. W. Inouye, T. E. X. Miller, R. Salguero-Gómez, A. M. Iler,  
350 and A. Compagnoni. 2021. Lagged and dormant season climate better predict plant vital  
351 rates than climate during the growing season. Global Change Biology 27:1927–1941.
- 352 Kassambara, A. 2023. Rstatix: Pipe-friendly framework for basic statistical tests.
- 353 Kress, J. 1990. The diversity and distribution of *Heliconia* (Heliconiaceae) in Brazil. Acta  
354 Botanica Brasileira 4:159–167.
- 355 Kress, W. J. 1983. Self-incompatibility systems in Central American *Heliconia*. Evolution  
356 37:735–744.

- <sup>357</sup> Kuss, P., M. Rees, H. H. Ægisdóttir, S. P. Ellner, and J. Stöcklin. 2008. [Evolutionary demography of long-lived monocarpic perennials: A time-lagged integral projection model.](#)
- <sup>358</sup>
- <sup>359</sup> Journal of Ecology 96:821–832.
- <sup>360</sup> Landau, W. M. 2021. The targets R package: A dynamic Make-like function-oriented
- <sup>361</sup> pipeline toolkit for reproducibility and high-performance computing. Journal of Open
- <sup>362</sup> Source Software 6:2959.
- <sup>363</sup> Levin, S. C., D. Z. Childs, A. Compagnoni, S. Evers, T. M. Knight, and R.
- <sup>364</sup> Salguero-Gómez. 2021. [Ipmr: Flexible implementation of Integral Projection Models in R.](#)
- <sup>365</sup> Methods in Ecology and Evolution 12:1826–1834.
- <sup>366</sup> Manly, B. F. 2018. Randomization, bootstrap and Monte Carlo methods in biology.
- <sup>367</sup> Chapman and Hall/CRC, New York.
- <sup>368</sup> Metcalf, C. J. E., S. P. Ellner, D. Z. Childs, R. Salguero-Gómez, C. Merow, S. M.
- <sup>369</sup> McMahon, E. Jongejans, et al. 2015. [Statistical modelling of annual variation for inference](#)
- <sup>370</sup> [on stochastic population dynamics using Integral Projection Models.](#) Methods in Ecology
- <sup>371</sup> and Evolution 6:1007–1017.
- <sup>372</sup> Molowny-Horas, R., M. L. Suarez, and F. Lloret. 2017. [Changes in the natural dynamics](#)
- <sup>373</sup> [of \*Nothofagus Dombeyi\* forests: Population modeling with increasing drought frequencies.](#)
- <sup>374</sup> Ecosphere 8:1–17.
- <sup>375</sup> Morris, W. F., and D. F. Doak. 2002. Quantitative conservation biology: Theory and
- <sup>376</sup> practice of population viability analysis. Sinauer, Sunderland, MA.

- <sup>377</sup> R Core Team. 2020. R: A language and environment for statistical computing. Vienna,  
<sup>378</sup> Austria <https://www.R-project.org/>.
- <sup>379</sup> Rees, M., D. Z. Childs, and S. P. Ellner. 2014. [Building integral projection models: A user's guide](#). Journal of Animal Ecology 83:528–545.
- <sup>381</sup> Rees, M., and S. P. Ellner. 2009. [Integral projection models for populations in temporally varying environments](#). Ecological Monographs 79:575–594.
- <sup>383</sup> ———. 2016. [Evolving integral projection models: Evolutionary demography meets eco-evolutionary dynamics](#). Methods in Ecology and Evolution 7:157–170.
- <sup>385</sup> Ribeiro, M. B. N., E. M. Bruna, and W. Mantovani. 2010. [Influence of post-clearing treatment on the recovery of herbaceous plant communities in Amazonian secondary forests](#). Restoration Ecology 18:50–58.
- <sup>388</sup> Römer, G., J. P. Dahlgren, R. Salguero-Gómez, I. M. Stott, and O. R. Jones. 2024. [Plant demographic knowledge is biased towards short-term studies of temperate-region herbaceous perennials](#). Oikos 2024:e10250.
- <sup>391</sup> Salguero-Gómez, R., O. R. Jones, C. R. Archer, Y. M. Buckley, J. Che-Castaldo, H. Caswell, D. Hodgson, et al. 2015. [The COMPADRE Plant Matrix Database: An open online repository for plant demography](#). Journal of Ecology 103:202–218.
- <sup>394</sup> Scott, E. R., M. Uriarte, and E. M. Bruna. 2022. [Delayed effects of climate on vital rates lead to demographic divergence in Amazonian forest fragments](#). Global Change Biology 28:463–479.

- <sup>397</sup> Stouffer, P. C., and R. O. Bierregaard. 1996. Forest fragmentation and seasonal patterns of  
<sup>398</sup> hummingbird abundance in Amazonian Brazil. *Ararajuba* 4:9–14.
- <sup>399</sup> Tenhumberg, B., E. E. Crone, S. Ramula, and A. J. Tyre. 2018. [Time-lagged effects of weather on plant demography: Drought and \*Astragalus scaphoides\*](#). *Ecology* 99:915–925.
- <sup>401</sup> Tuljapurkar, S. 1990. [Population dynamics in variable environments](#). (S. Levin, ed.).  
<sup>402</sup> Lecture Notes in Biomathematics (Vol. 85). Springer, Berlin, Heidelberg.
- <sup>403</sup> Tuljapurkar, S., C. C. Horvitz, and J. B. Pascalella. 2003. [The many growth rates and elasticities of populations in random environments](#). *The American Naturalist* 162:489–502.
- <sup>405</sup> Uriarte, M., M. Anciães, M. T. B. da Silva, R. Rubim, E. Johnson, and E. M. Bruna. 2011.  
<sup>406</sup> [Disentangling the drivers of reduced long-distance seed dispersal by birds in an experimentally fragmented landscape](#). *Ecology* 92:924–937.
- <sup>408</sup> Williams, J. L., H. Jacquemyn, B. M. Ochocki, R. Brys, T. E. X. Miller, and R. Shefferson.  
<sup>409</sup> 2015. [Life history evolution under climate change and its influence on the population dynamics of a long-lived plant](#). *Journal of Ecology* 103:798–808.
- <sup>411</sup> Williams, J. L., T. E. Miller, and S. P. Ellner. 2012. Avoiding unintentional eviction from  
<sup>412</sup> integral projection models. *Ecology* 93:2008–2014.
- <sup>413</sup> Wood, S. N. 2011. [Fast stable restricted maximum likelihood and marginal likelihood estimation of semiparametric generalized linear models](#). *Journal of the Royal Statistical Society Series B: Statistical Methodology* 73:3–36.

- <sup>416</sup> Xavier, A. C., C. W. King, and B. R. Scanlon. 2016. Daily gridded meteorological  
<sup>417</sup> variables in Brazil (1980–2013). International Journal of Climatology 36:2644–2659.



Description	Deterministic	Stochastic, kernel-resampled	Stochastic, parameter-resampled
Survival	$s(z)$	$s_y(z)$	$s(z; \theta_{0-36})$
Growth	$G(z'; z)$	$G_y(z'; z)$	$G(z'; z; \theta_{0-36})$
Flowering	$p_f(z)$	$p_{f_y}(z)$	$p_f(z; \theta_{0-36})$
Size-specific fecundity	$f(z)$	$f(z)$	$f(z)$
Germination & establishment	$g$	$g$	$g$
Seedling survival	$s_0$	$s_{0_y}$	$s_0(\theta_{0-36})$
Seedling growth	$G_0(z')$	$G_{0_y}(z')$	$G_0(z'; \theta_{0-36})$

**fig. 1.** Life cycle diagram of *Heliconia acuminata*. Each transition is associated with an equation for a vital rate function. The functions shown on the diagram correspond to those used to construct a general, density-independent, deterministic IPM. The table below shows the equivalent equations for stochastic, kernel-resampled IPMs and stochastic, parameter-resampled IPMs.

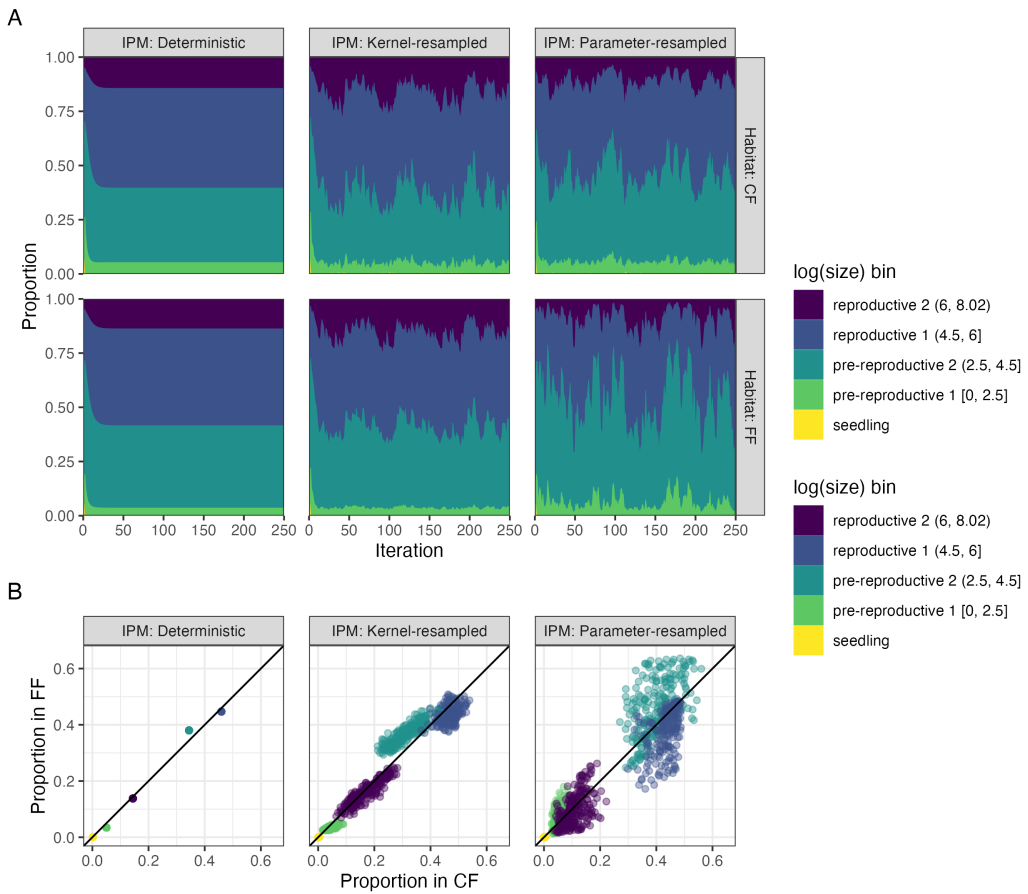


**fig. 2.** **(A)** The change over time in the the proportion of *Heliconia acuminata* populations in different size/stage classes when simulating population dyammics in Continuous Forest (CF) or Forest Fragment (FF) with three different integral projection models (e.g., IPMs). Results are shown for the first 250 iterations of populations; for the criteria used to define the size categories see Table 3. **(B)** The relative proportion of the population in each size class (FF vs. CF) for 250 iterations of each IPM model. Note that this excludes transient dynamics (iterations 1-30). Values on the 1-1 line indicate an iteration where CF and FF have the same proportion of the population in a given size class.

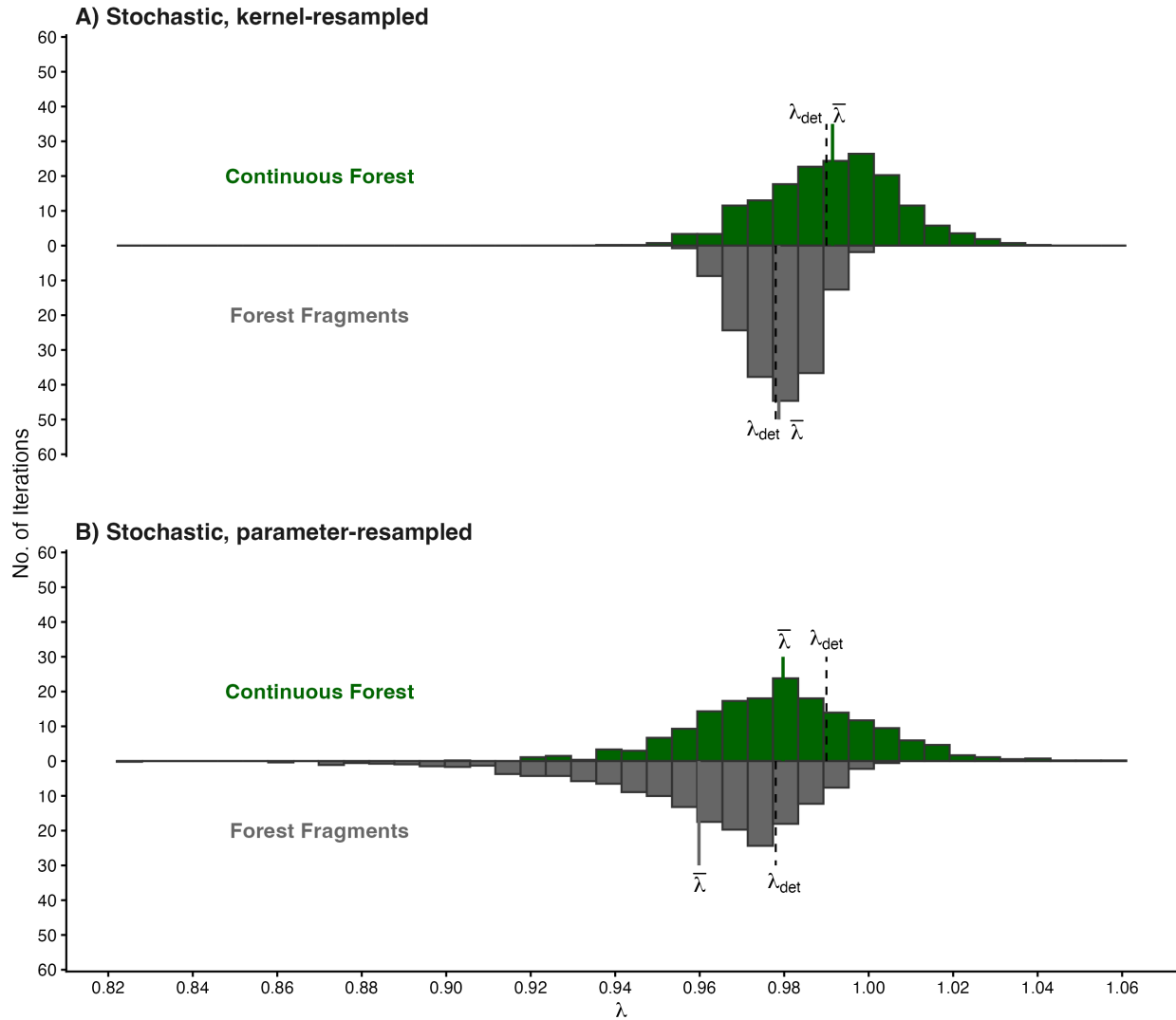


**fig. 3.** Distribution of 900 values of  $\lambda$  projected with (A) Stochastic, kernel-resampled IPMs and (B) Stochastic, parameter-resampled IPMs. IPMs were used to project  $\lambda$  for both Continuous Forest (above, in green) and Forest Fragments (below, in gray). The solid line indicates the mean value of  $\lambda$ , the dashed line indicates the value of  $\lambda$  in that habitat projected with Deterministic IPMs.

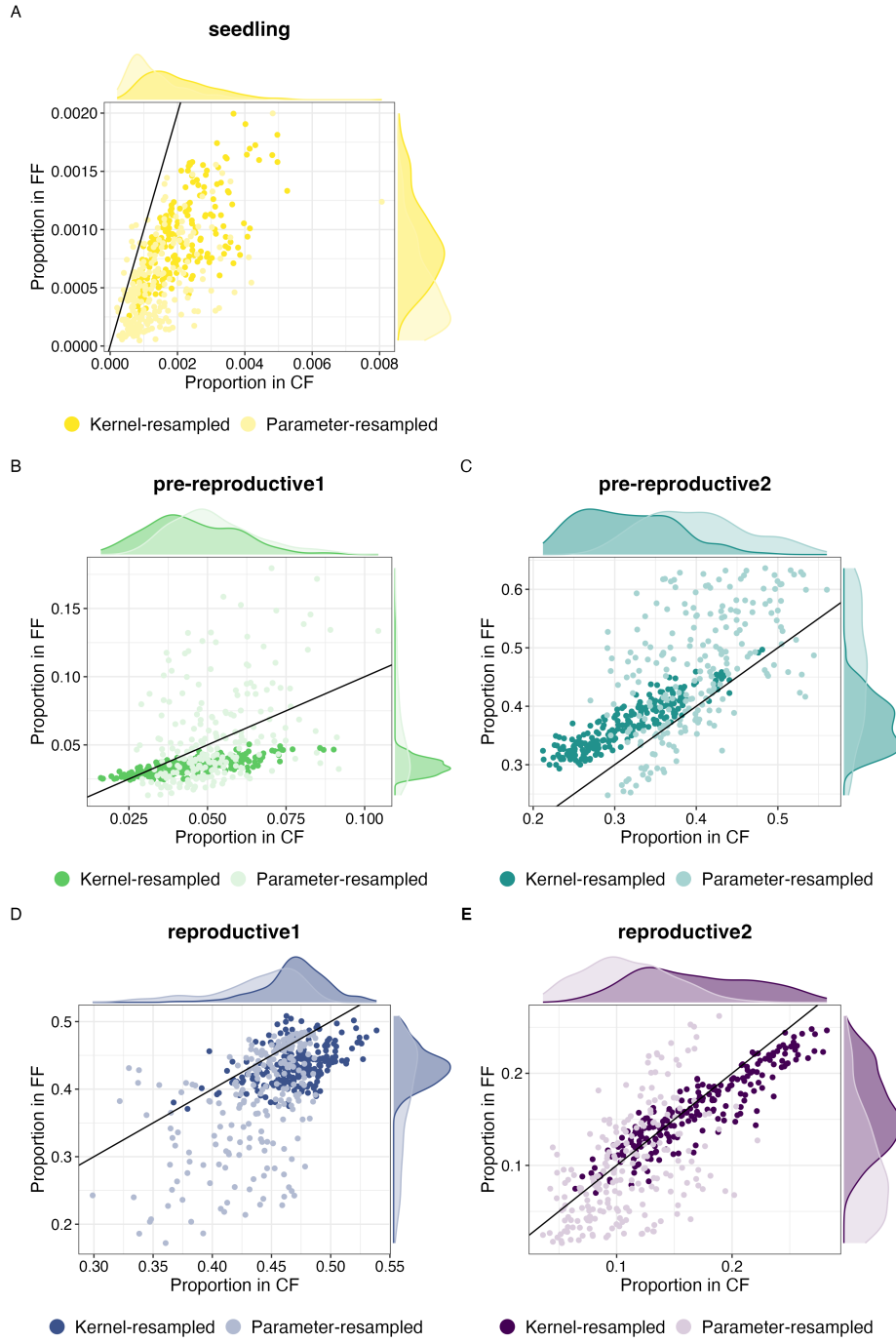


**fig. 4.** The relative proportion of the population in each size class (FF vs. CF) for each of 250 iterations of the kernel-resampled (dark shading) and parameter-resampled IPM models (light shading). Values on the 1-1 line indicate an iteration where CF and FF have the same proportion of the population in a given size class; the marginal plots indicate the distribution of these relative proportions for each class of IPM in each habitat. Note that both the scatterplots and marginal plots exclude transient dynamics (iterations 1-30).

Table 1: Comparison of vital rate models used to build IPM. The ‘Effect of Environment’ column describes how environmental effects were included in models. Those with ‘none’ were used to build deterministic IPMs; those with a random effect of year were used to build stochastic, kernel-resampled IPMs; and those with a distributed lag non-linear model (DLNM) were used to build stochastic, parameter-resampled IPMs. ‘*edf*’ is the estimated degrees of freedom of the penalized GAM.  $\Delta\text{AIC}$  is calculated within each habitat and vital rate combination.  $\Delta\text{AIC}$  within 2 indicates models are equivalent.

Habitat	Vital Rate	Effect of Environment	<i>edf</i>	$\Delta\text{AIC}$
<b>Continuous Forest</b>				
	Survival	Random effect of year	43.26	0.00
		DLNM	19.72	78.92
		None	4.98	260.01
	Growth	Random effect of year	78.43	0.00
		DLNM	23.87	158.46
		None	7.81	1896.03
	Flowering	DLNM	19.59	0.00
		Random effect of year	17.19	1.63
		None	7.47	381.86
	Seedling survival	None	1.00	0.00
		Random effect of year	1.82	1.39
		DLNM	4.01	1.53
	Seedling growth	Random effect of year	9.47	0.00
		DLNM	8.95	2.90
		None	1.00	172.33
<b>Forest Fragments</b>				
	Survival	DLNM	14.95	0.00
		Random effect of year	19.21	35.68
		None	4.33	51.25
	Growth	DLNM	25.18	0.00
		Random effect of year	37.84	199.98
		None	5.60	382.76
	Flowering	DLNM	20.61	0.00
		Random effect of year	13.81	27.40
		None	5.01	101.70
	Seedling survival	DLNM	5.57	0.00
		Random effect of year	5.09	5.72
		None	1.00	6.49
	Seedling growth	Random effect of year	6.25	0.00
		DLNM	8.18	2.29
		None	1.00	5.74

Table 2: Population growth rates for continuous forest (CF) and forest fragments (FF) under different kinds of IPMs with bootstrapped, bias-corrected, 95% confidence intervals.

IPM	Habitat	$\lambda$	95% CI (Lower, Upper)
<b>Deterministic</b>			
	FF	0.9778	(0.9736, 0.9823)
	CF	0.9897	(0.9877, 0.9920)
<b>Stochastic, kernel resampled</b>			
	FF	0.9787	(0.9735, 0.9835)
	CF	0.9913	(0.9892, 0.9939)
<b>Stochastic, parameter-resampled</b>			
	FF	0.9595	(0.9459, 0.9689)
	CF	0.9795	(0.9752, 0.9867)

Table 3: Size and stage categories used for comparing *Heliconia acuminata* population structure. Note that seedlings are a discrete size class not based on size (see *Methods* for additional details).

Category	Log(size)	Avg. prob. survival	Prob. flowering
Seedlings	-	-	-
Pre-reproductive 1	0–2.5	$\leq 0.9$	$\approx 0$
Pre-reproductive 2	2.5–4.5	$\geq 0.8$	$\approx 0$
Reproductive 1	4.5–6	$\geq 0.95$	$\leq 0.25$
Reproductive 2	$\geq 6$	$\geq 0.95$	$\geq 0.2$

Table 4: Results of statistical tests comparing the variance in the proportion of each habitat's population projected to be in each stage class by kernel-resampled vs. parameter resampled IPMs ( $N = 220$  projections per stage class). The variances for each habitat x stage class x IPM combination can be found in Table 5. Comparisons where the p-value of the test was  $< 0.05$  are indicated with an asterisk.

Stage	Habitat	Statistic	<i>df</i>	<i>P</i>
<b>Seedling</b>				
	CF	4.59	1	0.032*
	FF	11.51	1	0.001*
<b>Pre-reproductive 1</b>				
	CF	8.73	1	0.003*
	FF	96.13	1	< 0.0001*
<b>Pre-reproductive 2</b>				
	CF	0.99	1	0.319
	FF	39.67	1	< 0.0001*
<b>Reproductive 1</b>				
	CF	0.57	1	0.452
	FF	61.58	1	< 0.0001*
<b>Reproductive 2</b>				
	CF	0.11	1	0.745
	FF	18.78	1	< 0.0001*

Table 5: Summary statistics (median, mean, and variance) describing the proportion of populations projected to be in each of five life-history stages by kernel- and parameter-resampled IPMs (N = 220 projections for each IPM class x habitat combination.)

Stage	IPM	Median		Mean		Variance	
		CF	FF	CF	FF	CF	FF
<b>Seedling</b>							
	Kernel-resampled	0.0018	0.0009	0.0020	0.0020	0.000001	0.000000
	Parameter-resampled	0.0011	0.0004	0.0014	0.0014	0.000001	0.000000
<b>Pre-reproductive 1</b>							
	Kernel-resampled	0.0426	0.0340	0.0450	0.0450	0.000203	0.000034
	Parameter-resampled	0.0499	0.0438	0.0522	0.0522	0.000192	0.001167
<b>Pre-reproductive 2</b>							
	Kernel-resampled	0.3097	0.3677	0.3147	0.3147	0.003354	0.001884
	Parameter-resampled	0.3975	0.4613	0.4002	0.4002	0.003934	0.010380
<b>Reproductive 1</b>							
	Kernel-resampled	0.4725	0.4332	0.4704	0.4704	0.000736	0.000822
	Parameter-resampled	0.4464	0.4049	0.4371	0.4371	0.001481	0.006388
<b>Reproductive 2</b>							
	Kernel-resampled	0.1630	0.1554	0.1679	0.1679	0.002630	0.001745
	Parameter-resampled	0.1062	0.0882	0.1092	0.1092	0.001427	0.003213

Table 6: Estimated parameters, standard errors, t-values and P-values for the GLM of the effect of Habitat and IPM Type on projections of lambda.

Term	Estimate	SE	z value	P
(Intercept)	0.98	0	1568.20	< 0.0001
$Habitat_{FF}$	-0.02	0	-22.52	< 0.0001
$IPM_{Stoch}$	0.01	0	13.27	< 0.0001
$Habitat_{FF} : IPM_{Stoch}$	0.01	0	5.76	< 0.0001